Proceedings of the 9th International Conference on Physical Modelling in Coastal Engineering (Coastlab24)

Delft, Netherlands, May 13-16, 2024

Conference Paper, DOI: 10.59490/coastlab.2024.694

COMPARATIVE GRASS PULLOUT TESTS AND WAVE OVERTOPPING SIMULATIONS ON THREE SPECIES-RICH GRASS COVERED DIKES IN THE NETHERLANDS

RENS VAN DER MEIJDEN[1], GOSSE JAN STEENDAM[2], ROY MOM[3], ANDRÉ VAN HOVEN[4], JORD WARMINK[5], DENIE AUGUSTIJN[6]

1 University of Twente, Enschede, The Netherlands, E-mail: r.vandermeijden@utwente.nl

2 Infram Hydren, Maarn, The Netherlands, E-mail: gosse.jan.steendam@infram-hydren.nl

3 Infram Hydren, Maarn, The Netherlands, E-mail: roy.mom@infram-hydren.nl

4 Deltares, Delft, The Netherlands, E-mail: Andre.vanHoven@deltares.nl

5 University of Twente, Enschede, The Netherlands, E-mail: j.j.warmink@utwente.nl

6 University of Twente, Enschede, The Netherlands, E-mail: d.c.m.augustijn@utwente.nl

ABSTRACT

Grass cover erosion by wave overtopping is a major failure mechanism for earthen dikes. Grass cover erosion resistance (represented by the critical velocity, U_c) can be assessed using full-scale, destructive tests with the wave overtopping simulator (WOS) in combination with the erosion model 'cumulative overload method' (COM). Although these tests provide valuable information, they are relatively expensive and time consuming. Therefore, a small-scale grass pullout test (GPT), which translates the vertical pullout force of a grass sod to a U_c, may be an attractive alternative. In this paper, based on comparative testing with the WOS and GPT on three species-rich grass covers on dikes in the Netherlands, we assess the correspondence between the U_c obtained with the WOS and GPT for species-rich grass covers. Ultimately, by also including historical tests, we aim to get more insight into the suitability of the GPT for quantitative erodibility assessment of grass covers in general.

During testing with the WOS, no failure was observed for the tested grass cover sections. Therefore only a lower bound of the U_c could be derived. Results indicate that the estimated U_c with the GPT is around the lower bound values obtained with the WOS. This is in line with previous tests on conventional grass covers, for which the GPT provides a more conservative estimate of the U_c than the WOS. Adaptations in the translation from pullout force to U_c may correct for the negative bias and hence improve the reliability of the GPT for quantitative erodibility assessment. Several suggestions to adapt the GPT in future work are provided in this paper. These adaptations should be tested and validated for conventional as well as species-rich grass covers to guarantee the general applicability of the method.

KEYWORDS: Wave Overtopping, Dikes, Grass Covers, Grass Pullout Test, Critical Velocity

1 INTRODUCTION

Earthen dikes in the Netherlands typically comprise a clay or sand core, with a clay(ey) substrate on top wherein grassland vegetation is rooted. This clayey substrate with grassland vegetation is referred to as a grass cover, and it protects the body of the dike against erosion by waves. Grass cover erosion by wave overtopping is one of the major failure mechanisms for these earthen dikes, particularly for sea and lake dikes (Van der Meer et al., 2018; Van Bergeijk et al., 2020). The erosion resistance of the grass cover, represented by the critical velocity, U_c, is a determining factor for the required crest height in the design of a dike. Hence, to ensure the required safety level is met, the erosion resistance of the grass cover is of vital importance.

Field assessment of grass cover erosion resistance in the Netherlands and other countries has been done using full-scale, destructive testing with the wave overtopping simulator (WOS) in combination with the cumulative overload method (COM). However, full-scale testing with the WOS is relatively expensive and time consuming. Hence, the use of a small-scale grass pullout test (GPT), which estimates the U_c via the pullout force of a grass sod, may be an attractive alternative. Moreover, due to its mobility and ease of use, its results may serve a wider range of applications, such as correlating grass cover strength to soil and vegetation data. The WOS is regarded as the most reliable method to find the U_c and has been successfully applied at various grass cover types for a long time. During previous tests, the correspondence between the U_c from the GPT and WOS has been good at five initial test plots with grassland vegetation on a clayey substrate (Bijlard et al., 2017). However, more recent tests on a sandy substrate indicated significant differences between the results of both methods.

In Future Dikes, an innovation project funded by the Dutch Flood Protection Programme (in Dutch:

Hoogwaterbeschermingsprogramma, HWBP), the required knowledge for the nation-wide application of species-rich grass covers is developed. As part of the project, a field campaign was set up to assess the erosion resistance of existing species-rich grass covered dikes in the Netherlands (Radboud University, 2023). The field campaign included tests with both the WOS (3 sites) and GPT (20 sites). However, given previous results, it was unknown whether the GPT was applicable to reliably estimate the U_c of these species-rich grass covers, which typically comprise a relatively sandy substrate. In this paper, through comparative testing with the GPT and WOS at three sites where both methods were applied, we analyse the correspondence between their results. Ultimately, by including tests on both conventional as well as species-rich covers, we aim to get a comprehensive insight into the applicability of the GPT for quantitative erodibility assessment of grass covers.

2 DATA AND METHODS

2.1 Wave overtopping erosion and the cumulative overload method

Grass covers on landward and seaward slopes of dikes typically consist of a densely rooted top layer on a substrate of (sandy) clay. One of the main failure mechanisms for these grass covers is erosion by wave run-up or wave overtopping. The pulsating load on the grass cover is caused by high flow velocities of the wave front resulting in shear stresses and pressure gradients at the surface. These gradients induce grass cover erosion by washing out material, stripping off the turf (i.e. the grass sod) and eventually breaking through the top layer. After this initial breakthrough, degradation of the top layer and the substrate may increase fast. This is defined as grass cover failure (Steendam et al., 2012). The cumulative overload method (COM), as given in Equation (1), may be used to predict the extent of grass cover erosion as a result of wave overtopping and wave run-up (Van der Meer et al., 2017; Hoffmans et al., 2018; Van der Meer et al., 2020).

$$D = \sum_{i=1}^{N} (U_i^2 - U_c^2) \quad \text{For } U_i^2 > U_c^2 \tag{1}$$

where the extent of damage is quantified by a damage number D (m^2/s^2), U_i is the wave front velocity, U_c is the critical velocity and N is the number of wave volumes. Note that, in this paper, the influence factors for transitions and objects, α_s and α_M, and the accelerations factor, α_a, are left out since transitions and objects are not considered and the front velocities were directly measured.

The damage number D increases when U_i exceeds U_c. This means that mainly the large overtopping volumes contribute to D. Based on previous tests in the Netherlands, for a D of 1000 m^2/s^2, 4000 m^2/s^2 and 7000 m^2/s^2 the COM predicts the damage criteria 'initial damage', 'several open spots' and 'cover failure', respectively (Van der Meer et al., 2020). However, the method was calibrated to predict failure. Prediction of damage before failure is often not accurate.

In this paper, two methods were applied to determine the U_c of species-rich grass covers. First, through full-scale simulations with the WOS in combination with the COM, the U_c can be derived from (non-)failure and the extent of cover damage. Second, using a small-scale GPT, the U_c can be estimated from the pullout force of a grass sod.

2.2 The wave overtopping simulator

The wave overtopping simulator (WOS), as seen in Figure 1, was designed and constructed in 2006 and has since then been used for destructive testing of grass cover erodibility in the Netherlands, Belgium, Vietnam, the US and Singapore (Van der Meer et al., 2007; Le Hai Trung et al., 2011; Thornton et al., 2013; Van der Meer et al., 2020).

Figure 1 The wave overtopping simulator in action.

With this method, a 20 m^3 specially designed container is placed on top of the dike crest and subsequently filled with water. Individual wave volumes are then released through drawer valves and guided down the slope over a section of 4 m wide (Van der Meer et al., 2020). Two sections were tested for all three sites.

The wave volumes, randomly released at the crest, represent the waves overtopping the dike during the peak of a storm. The individual overtopping volumes follow a Weibull distribution, which is derived using the procedure in the EurOtop manual 2018 (Van der Meer et al., 2018). Using the variables in Table 1, six test scenarios were constructed. For each test, the corresponding wave volumes were released in appearing order over the test sections.

Table 1 Wave overtopping (WO) scenarios constructed with a differing average overtopping discharge (q), freeboard (R_c), significant wave height (H_s), peak wave period (T_p), wave steepness (s), number of overtopping waves (N_{ow}) and probability of overtopping (P_{ov}).

Test	q (l/s/m)	R_c (m)	H_s (m)	T_p (s)	s (-)	N_{ow} (-)	P_{ov} (-)
WO-1-1	1	1.94	1.0	3.58	0.05	437	0,07
WO-10-1	10	1.25				2,048	0,34
WO-50-1*	50	0.68				4,376	0,73
WO-100-1	100	0.39				5,432	0,90
WO-50-2	50	2.45	2.0	5.66	0.04	1,658	0,43
WO-100-2**	100	1.90				2,303	0,60

** This test was only used for one of the sections. See section 4.2.*

*** This test was repeated for every section.*

It is important to note that, due to the time required for opening and closing the valves in combination with the filling discharge of the container, there is a minimum volume which can be released for each test. In order to release the same total volume as for the theoretical distributions in Table 1, the volumes that were too small to simulate were added up and divided by the minimum volume. This means that the number of released wave volumes equals roughly 50-80 percent of N_{ow} in Table 1. Figure 2 shows the wave volume distributions for each scenario. The distributions are cut off at the maximum capacity of the simulator (4.7 m^3/m) as well as the minimum volume per scenario (dashed line).

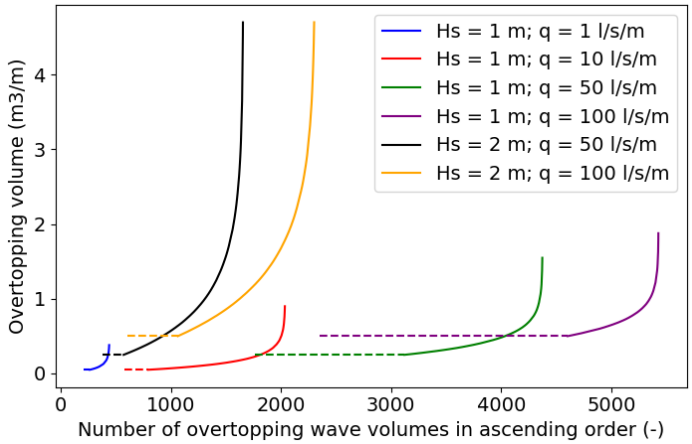

Figure 2 Wave volume distributions used for the wave overtopping simulations.

For various pre-defined wave volumes, the front velocity was measured using either a drone or an action camera, which was placed on a pole next to the test section. The video material comprises the entire test section as well as the markers which were placed at every metre along the test section. The front velocity along the slope was estimated by counting the number of video frames it took for the wave front to move 1 m. To reduce noise, a smooth line was fitted through the discrete measurements, which was eventually used to get a continuous front velocity profile along the slope. This velocity profile represents the wave load (i.e. U_i^2) in the COM.

By visually keeping track of the initiation and development of damage to or failure of the grass cover, the value of D is approximated (i.e. 1000, 4000 or 7000 m^2/s^2). The cumulative wave load can be determined based on the front velocities. From various options for the U_c, the 'correct' estimate is the one which results in a D matching the observed damage threshold during the simulation. This procedure is described in more detail in Van der Meer et al. (2020). Since the COM is calibrated for predicting failure, the threshold of 7000 m^2/s^2 is considered normative in estimating the U_c. This means that, in case the grass cover does not fail, a lower bound of the U_c can be derived.

2.3 The grass pullout test

The grass pullout test (GPT), as seen in Figure 3, was developed and applied on a series of grass on clay dikes in 2015, for which it estimated a U_c similar to the U_c found with the WOS (Bijlard et al., 2017). The device consists of a tripod, which connects a 0.2 x 0.2 m^2 metal pull frame to an electric motor via a cylinder. The pull frame is attached to the turf through five metal pins at 0.04 m below the surface. A sod is then pulled out at a constant speed of 1 cm/s, while the required tensile force and displacement are recorded. The maximum tensile force occurs at failure of the sod. At this stage, the upward pull force exceeds the combination of resistant downward forces (i.e. from sod weight, soil cohesion and roots).

Figure 3 The grass pullout test in action.

Typically, 40 tests are performed within a test plot of 15 x 10 m^2, of which 30 with two (opposite) sides and 10 with four sides cut free. The average maximum tensile force of the 2-sided ($\overline{F_2}$) and 4-sided ($\overline{F_4}$) tests is used to derive an amplification factor (*AF*):

$$AF = 1.1\left(\frac{\overline{F_2} + (\overline{F_2} - \overline{F_4})}{\overline{F_2}}\right) \tag{2}$$

which translates F_2 to the tensile force of an intact sod (F_i):

$$F_i = AF * F_2 \tag{3}$$

Then, the tensile force of the intact sod is divided by the sum of the area of the bottom (A_b), the free and attached sides (A_{s1} and A_{s2}) of the pulled sod, which gives a critical normal stress ($\sigma_{grass,c}$) for each of the 30 2-sided tests:

$$\sigma_{grass,c} = \frac{F_i}{A_b + 2 * A_{s1} + 2 * A_{s2}} \tag{4}$$

The spatial distribution of $\sigma_{grass,c}$ within the test plot may provide insight into the spatial heterogeneity of the grass cover strength, which is more difficult to assess using the WOS.

Now, by assuming the pressure fluctuations in the top layer as the main loading mechanism during wave overtopping, $\sigma_{grass,c}$ can be written in terms of velocity. By working out the balance of the vertical forces acting on a conceptual turf element, using the equation of motion, the definition of bed shear stress as well as the exponential decrease of the root density with depth, Hoffmans et al. (2009) and Hoffmans (2012) derived a formula for the U_c of a grass cover:

$$U_c = \alpha_{grass,U} r_0^{-1} \sqrt{\frac{\psi_c(\sigma_{grass,c}(0) - p_w)}{\rho}} \tag{5}$$

where $\alpha_{grass,U}$ (-) is a factor with value 2.0, r_0 is the relative turbulence intensity (-) with an approximate value of 0.12 for wave overtopping conditions on a grass slope, ψ_c is the critical Shields parameter (-) with a value of 0.03, p_w is the suction pressure (N/cm^2) in the topsoil, ρ is the water density (kg/m^3) with a value of 1000, and $\sigma_{grass,c}(0)$ is the critical normal stress (N/cm^2) at the ground level (Hoffmans, 2012; Hoffmans et al., 2018). Since experiments are typically done in autumn or winter, in wet conditions, it is assumed that p_w is negligible. This way, $\sigma_{grass,c}(0)$ is the only variable parameter.

For $\sigma_{grass,c}(0)$, it is assumed that, in case of wave overtopping erosion, the grass cover will most likely fail at the weakest spot in the test plot. It is assumed that the 30 values of $\sigma_{grass,c}$ per plot are sampled from a normal distribution. Based on the mean and standard deviation of these 30 samples, the 2.5th percentile value is assumed as representative for the weakest spot. The 2.5th percentile value is then used in Equation (5) to estimate the U_c (Bijlard et al., 2017).

3 TEST SITES

In the Future Dikes project, the GPT and WOS were used at three existing species-rich grass covered dikes along the Meuse River, a few kilometres south-west of Nijmegen, in the east of the Netherlands, as seen in Figure 4.

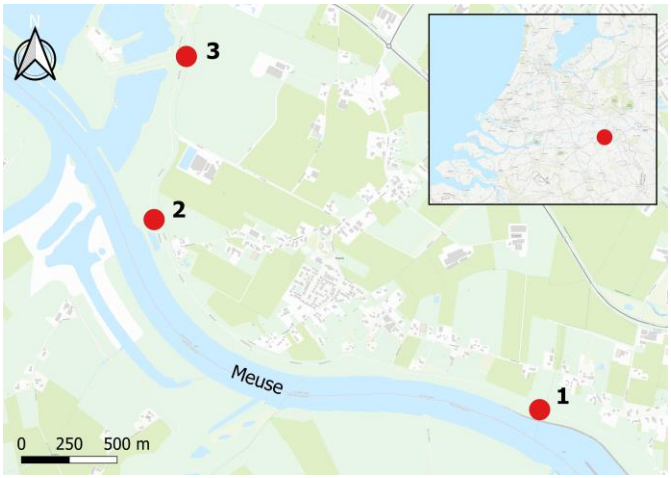

Figure 4 Location of test sites 1, 2 and 3.

General characteristics regarding the slope geometry and the orientation of each section per site are summarised in Table 2.

Table 2 Characteristics of slope geometry and orientation.

	Site 1		**Site 2**		**Site 3**	
	Section 1	*Section 2*	*Section 1*	*Section 2*	*Section 1*	*Section 2*
Slope length (m)	14		13		12	
Average steepness (m vert.: m hor.)	1:3.5	1:3.2	1:3.2		1:4	1:3.2
Steepest part of the slope m vert.: m hor. (at m distance from crest)	1:2.3 (3-4)	1:2.2 (4-5)	1:2.7 (6-7)	1:2.6 (10-11)	1:2.6 (0-1)	1:2.1 (0-1)
Orientation	South-west		South-west		South-east	
Inside/outside slope	Outside		Outside		Inside	

For these three sites, the first set of GPTs was carried out in October 2022, while the tests with the WOS were carried out from January to March 2023. Additional GPTs, 8 sets of 5 tests over 350 m of dike length, near site 3 were done in November 2022 to analyse the spatial variability of grass cover strength. Additional GPTs at sites 1-3 were done in January and February 2023, together with the WOS, to study the temporal variability of grass cover strength. An overview of the measurements is given in Table 3.

Table 3 Measurements at sites 1, 2 and 3 in October (O), November (N) 2022 and January (J), February (F), and March (M) 2023.

	Site 1		**Site 2**		**Site 3**		
	O22	*J23*	*O22*	*F23*	*O22*	*N22*	*FM23*
Wave overtopping simulation (WOS)		x		x			x
Grass pullout test (GPT)	x	x	x	x	x	x	x

4 RESULTS OF THE WAVE OVERTOPPING SIMULATIONS

4.1 Front velocities

To obtain a continuous front velocity profile (i.e. wave load) along the slope, the front velocities derived from the discrete video frames were first averaged for two repeated volumes. Then, a trendline was fitted through the resulting graphs at separate sections of the slope, as seen in Figure 5. The fitted trendline was used as input for the COM.

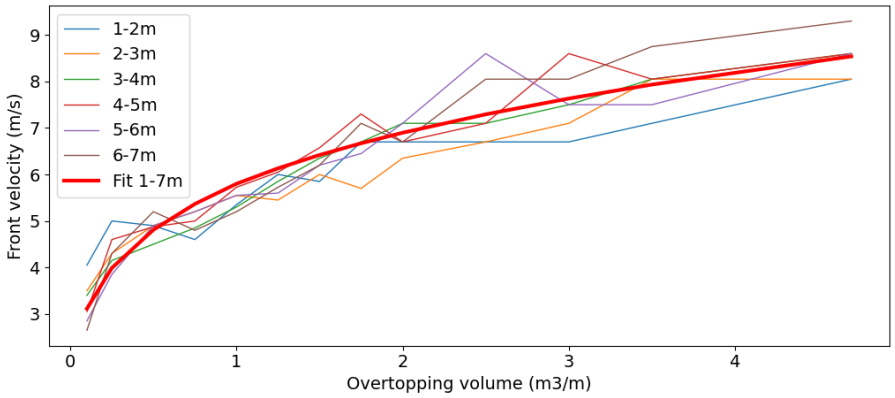

Figure 5 Measured front velocities for section 2-1 at 1-7 m from the crest, including fitted trendline.

For all sites, the front velocity increases with the wave volume. For site 1 and 2, the front velocities increased towards the toe, such that the highest cumulative wave load occurred at the lower half of the slope, roughly at a distance of 8-12 m from the crest. However, for site 3, the highest flow velocities occurred at the upper slope, at a distance of 2-5 m from the crest. This may be explained by the fact that the first part of the upper slope at site 3 is relatively steep, whereas the lower slope is more gradual.

4.2 Observed grass cover damage during overtopping simulations

Table 4 contains the observed damage per section. For the observed damage, also the moment and the location at the slope are given.

Table 4 Observed damage per test section. Section 1-1 refers to site 1, section 1.

Section	Test	Moment/ duration	Distance from crest (m)	Extent of damage
1-1	WO-1-1, WO-10-1, WO-100-1	15 h		No damage
	WO-50-2	After 1-2 h 3 h	5-6 5-9	Start of damage Turf stripped off + 3.2 m
	WO-100-2	5 h	6-11	Turf stripped off + 2.3 m
	WO-100-2 (rep.)	4.5 h	6-12	Turf stripped off + 1.7 m,
1-2	WO-1-1, WO-10-1, WO-100-1, WO-50-2	20 h		No damage
	WO-100-2	After 1-2 h	4	Initial damage
		3h		Turf stripped off + 1.15 m
	WO-100-2 (rep.)	5 h		Turf stripped off + 0.5 m, no failure
2-1	WO-1-1, WO-10-1, WO-100-1, WO-50-2	20 h		No damage
	WO-100-2	After 2h		Damage at crest transition
	WO-100-2 (rep.)	5h	0-7	Turf stripped off + 7 m , no failure
2-2/ 3-1/ 3-2	WO-1-1, WO-10-1, WO-100-1, WO-50-2	30h		No damage
	WO-100-2, WO-100-2 (rep.)			
3-2*	WO-10-1, WO-50-1, WO-50-2, WO-100-2	18 h		No damage

** Additional testing for transition asphalt-slope. The WO-100-2 test was only done for three hours*

Although the simulated wave volumes induced significant grass cover erosion, none of the covers failed. Initial damage to the (upper) slope was observed only for sections 1-1 (i.e. site 1, section 1) and 1-2. For section 2-1 the damage initiated at the transition from the asphalt road to the slope. After the initial damage occurred, the remaining wave volumes stripped of large parts of the densely rooted turf, as seen Figure 6.

Figure 6 Example of stripped-off turf over roughly 3 m at section 1-1.

Although the areal extent of the cover damage at sections 1-1, 1-2, and 2-1 was significant, the removal of the turf did not initiate any further erosion of the clayey substrate with roots below. Since the exposed substrate still contained some roots, it is considered a part of the grass cover. As a result, neither of these sections reached cover failure. For sections 2-2, 3-1 and 3-2 the performed tests did not initiate any damage to the grass cover. Section 3-2 was tested for an additional 18 hours to specifically test the strength of the asphalt-slope transition. Neither the transition nor the grass cover suffered any damage. The extra load from the additional testing was also included in the derivation of the U_c.

4.3 Derivation of U_c using the observed damage and the cumulative overload method

For each section, a U_c was derived for the damage thresholds 'initial damage' and 'cover failure' of the COM, as seen in Table 5. For site 1, the threshold 'initial damage' can be traced back to a single moment during the simulation. Therefore also a specific damage number and U_c can be derived. For 'cover failure', the damage number at the end of the simulation is used since failure was not observed for either of the sites. A lower bound value of U_c is given when no damage or no failure was observed. Deriving a damage number for 'several open spots' is not possible. After 'initial damage', the turf layer was stripped off over large areas as the overtopping waves volumes hit the lower side of the erosion hole. Hence, damage was not initiated at separate locations of the cover. The threshold 'several open spots' was therefore not observed and is left out in Table 5.

Table 5 U_c values per section for the damage thresholds 'initial damage' and 'no failure'.

	Site 1		**Site 2**		**Site 3**	
	Section 1	*Section 2*	*Section 1*	*Section 2*	*Section 1*	*Section 2*
U_c – initial damage, during simulation (m/s) D = 1000 m²/s²	*5.7*	*7.2*	*-**	*> 7.8*	*> 8.5*	*> 7.9*
U_c – no failure, end of simulation (m/s) D = 7000 m²/s²	**> 7.4**	**> 7.2**	**> 6.8**	**> 6.4**	**> 6.9**	**> 6.7**

** Damage was not initiated at the slope.*

Of the three damage thresholds, the COM is most accurate in predicting cover failure. Hence the lower bound U_c at the end of the simulation is considered normative. For sections 1-1 and 1-2, the U_c from 'no failure' is equal to or greater than the U_c from 'initial damage'. For sections 2-2, 3-1 and 3-2 the U_c from 'no failure' is lower than the U_c from 'initial damage', which is due to the proportionality of D and U_c^2 (i.e. when U_i is known, a lower D gives a higher U_c) see Equation (1).

Note that, despite 18 hours of additional testing at section 3-2, the lower bound U_c is lower than at section 3-1. This is explained by the lower measured front velocities and the fitted trendline for section 3-2 compared to section 3-1.

5 RESULTS OF THE GRASS PULLOUT TESTS

5.1 Maximum tensile force, amplification factor and sod dimensions

Table 6 shows the tensile forces (F_2, F_4 and F_i), the *AF* and the sod dimensions for the 2-sided tests at sites 1, 2 and 3.

Table 6 Average maximum tensile forces (F_2, F_4, F_i *in* N) including variation coefficient, CV (-), amplification factors, *AF* (-) and average sod dimensions (width and thickness in cm) including variation coefficient, CV (-), for sites 1, 2 and 3.

	Site 1		Site 2		Site 3		
	O22	*J23*	*O22*	*F23*	*O22*	*N22*	*FM23*
Tensile force, F_2 (N) – average (CV)	892 (0.24)	1032 (0.17)	909 (0.15)	983 (0.16)	821 (0.19)	877 (0.16)	934 (0.14)
Tensile force, F_4 (N) – average (CV)	647 (0.12)	682 (0.19)	649 (0.15)	587 (0.10)	543 (0.15)	544 (0.18)	585 (0.18)
***AF* (-)**	1.40	1.47	1.41	1.54	1.47	1.52	1.51
Tensile force, F_i (N) – average (CV)	1253 (0.24)	1520 (0.17)	1287 (0.15)	1517 (0.16)	1209 (0.19)	1332 (0.16)	1411 (0.14)
Sod width (cm, n=30) – average (CV)	28.0 (0.16)	26.1 (0.10)	25.8 (0.07)	25.4 (0.09)	27.0 (0.10)	26.1 (0.11)	25.8 (0.12)
Sod thickness (cm, n=30) – average (CV)	8.7 (0.20)	9.0 (0.19)	8.2 (0.17)	9.4 (0.19)	9.5 (0.21)	10.1 (0.15)	9.9 (0.22)

The difference between F_2 and F_4 determines *AF*, which varies roughly between 1.40 and 1.55. A low *AF* (i.e. small difference between F_2 and F_4) corresponds to a relatively strong contribution of the bottom of the sod/vertical roots, whereas a high *AF* (i.e. large difference between F_2 and F_4) corresponds to a relatively strong contribution of the sides/horizontal roots.

Note that the average width of the pulled sod is larger than the width of the pull frame (20 cm). The average thickness differs roughly between 8-10 cm.

5.2 Critical normal stress and critical velocity

Table 7 shows the results regarding the critical normal stresses ($\sigma_{grass,c}$) and U_c from the GPT at sites 1-3.

Table 7 Average critical normal stress ($\sigma_{grass,c}$, in N/cm^2) including variation coefficient, CV (-), skewness of $\sigma_{grass,c}$ (-) and U_c (m/s) for sites 1, 2 and 3.

	Site 1		Site 2		Site 3		
	O22	*J23*	*O22*	*F23*	*O22*	*N22*	*FM23*
Critical normal stress, $\sigma_{grass,c}$ (N/cm^2) – average (CV)	1.1 (0.25)	1.4 (0.18)	1.2 (0.17)	1.3 (0.24)	1.0 (0.20)	1.1 (0.20)	1.2 (0.23)
Skewness of $\sigma_{grass,c}$	0.6	1.2	-0.4	-0.3	0.6	-0.1	1.3
U_c (m/s)	6.1	7.7	7.2	6.8	6.5	6.8	6.7

Note that the U_c depends on both the average $\sigma_{grass,c}$ and the standard deviation, which together determine the distribution of $\sigma_{grass,c}$. The average F_i and $\sigma_{grass,c}$ provide a rough indication of the erosion resistance of the cover. However, the presence of weak spots, which increases the spread of F_i and $\sigma_{grass,c}$, also heavily affects the U_c. This is clear when comparing plots 2-O22 to 2-F23. The latter has a higher average $\sigma_{grass,c}$, but also a higher *CV*, which gives a lower U_c.

The assumption of the 2.5th percentile of $\sigma_{grass,c}$ as a measure of the weakest spot per plot is based on a normal distribution of $\sigma_{grass,c}$. However, the skewness values indicate that the 30 samples of $\sigma_{grass,c}$ are not always near 0, like for a normal distribution. Four test plots have a positive (right) skew, whereas two have a negative (left) skew. Only one plot (3-N22) has a skew which is near 0. The skewness of the sample distribution may have consequences for the suitability of the 2.5th percentile to represent the weakest spot, as further explained in the Discussion section.

The U_c for sites 2 and 3 does not differ significantly per plot. Apart from plot 3-N22 (i.e. 8 smaller plots over 350 m of dike length to study spatial variation), the plots at sites 2 and 3 were not located far apart (distance ~ 10-20 m). In contrast, the results for plots 1-O22 and 1-J23 differ significantly, which may partly be explained by the larger distance (~ 80 m) between the plots.

6 DISCUSSION

6.1 Correspondence of the critical velocity determined by WOS and GPT for species-rich grass covers

For the GPT to be a viable tool for grass cover erodibility assessment, the estimated U_c needs to correspond with the U_c found with the WOS. Table 8 summarizes the U_c values obtained with the GPT and WOS for sites 1, 2 and 3 in Future Dikes. For the WOS the lower-bound value, corresponding to the damage threshold 'no failure', is normative.

Table 8 Comparison of the U_c from the GTP and the WOS for sites 1, 2 and 3.

	Site 1		**Site 2**		**Site 3**			**Average**
	O22	*J23*	*O22*	*F23*	*O22*	*N22*	*FM23*	
U_c – GPT (m/s)	6.1	7.7	7.2	6.8	6.5	6.8	6.7	***6.8***
U_c – WOS (no failure) (m/s)	*Section 1*	*Section 2*	*Section 1*	*Section 2*	*Section 1*	*Section 2*		
	> 7.4	> 7.2	> 6.8	> 6.4	> 6.9	> 6.7		***> 6.9***

The results indicate that the U_c obtained with the GPT is mostly equal to or just above the lower bound U_c determined with the WOS. Only for plots 1-O22 and 3-O22, the U_c with the GPT is lower than the U_c with the WOS. Since no failure was observed during the overtopping simulations, the real value of U_c cannot be determined. However, given the absence of both damage and failure after the wave overtopping test, it is likely that U_c is higher than the current values in Table 8. In that case, the GPT would provide a conservative estimate of the U_c for these species-rich grass covers.

When considering only the U_c obtained with the GPT which were done at the same time and location as the WOS (i.e. 1-J23, 2-F23 and 3-FM23), the qualitative results of both methods seem to correspond reasonably well. The estimated U_c with the GPT for plot 1-J23 is significantly higher than for plots 2-F23 and 3-FM23. Comparably, the lower bound U_c for site 1 with the WOS is higher than for sites 2 and 3 due to the higher front velocities. Furthermore, the difference between the U_c for plots 2-F23 and 3-FM23 is small, which also applies to the lower bound U_c derived from the WOS. It is however difficult to draw definitive conclusions since the real value of U_c with the WOS is unknown.

6.2 Correspondence of the critical velocity determined by WOS and GPT for conventional grass covers

Since 2015, the GPT has been tested on conventional grass covers with both clayey and sandy substrates. Bijlard et al. (2017) reported a good correspondence between the U_c obtained with the GPT and WOS for grass on clay. However, during more recent tests, the GPT was not as reliable for grass on sand (Van Hoven, 2022). Since the dimensions of the pulled out sod may vary significantly, one adaptation to the GPT for the more recent tests (after 2018) was the use of the real sod dimensions (*width* x *20* x *thickness* cm^3, see Table 6) for the derivation of $\sigma_{grass,c}$, instead of the default dimensions (20x20x8 cm^3) used by Bijlard et al. (2017). To analyse the accuracy of the current GPT for grass on clay, the tests by Bijlard et al. (2017) were recalculated using the real sod dimensions. The results are included in Figure 7, which shows the U_c obtained with the current GPT plotted against the U_c obtained with the WOS for all sites where both methods were applied in the past. These include conventional grass covers on clay (9 sites) and sand (7 sites), as well as our species-rich covers (3 sites). For the latter, the GPTs in the winter of 2023 and the highest minimum U_c are used for the GPT and WOS results, respectively. For comparison, also the test results in Bijlard et al. (2017) are indicated.

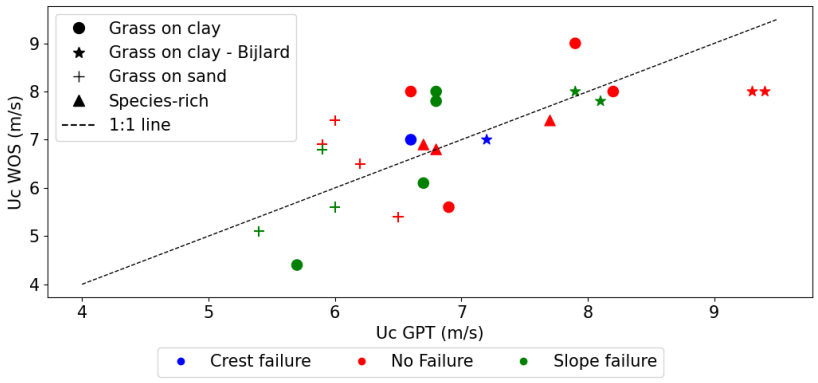

Figure 7 U_c obtained with the grass pullout test plotted against U_c obtained with the wave overtopping simulator.

Despite the fact that most points in Figure 7 are distributed around the 1:1 line, a close examination of the results indicates significant discrepancies between the U_c obtained with the GPT and WOS. For only four out of eleven sites where 'no failure' was observed (i.e. red dots), the U_c obtained with the GPT exceeds the lower bound U_c obtained with the WOS. For five out

of eight sites where either 'crest failure' or 'slope failure' was observed, there is a reasonable correspondence between both methods. However, considering 'slope failure', the GPT still significantly underestimates the highest (~ 8 m/s) and overestimates the lowest (~ 4.5 m/s) U_c obtained with the WOS.

Given the tests with the GPT and WOS were never done at exactly the same time and location, the results in Figure 7 may be affected by spatial and temporal variation of grass cover strength. To mitigate the effect of spatial and temporal variation, the statistics based on all previous tests with the GPT and WOS for a certain cover type can be compared, as seen in Table 9. The median is used to measure central tendency due to the relatively small data sets and the presence of outliers.

Table 9 Median ± standard deviation of the U_c (m/s) for grass on clay/sand and species-rich covers based on the current GPT and WOS. The number of available sites (n) per method is given between brackets.

	Grass on clay	Grass on sand	Species-rich
Grass pullout test (GPT)	7.1 ± 0.9 (n=17)	5.9 ± 0.6 (n=14)	6.7 ± 0.9 (n = 20)
Wave overtopping simulator (WOS	8.0 ± 1.3 (n=13)	6.1 ± 1.2 (n = 10)	> 6.9 ± 0.3 (n = 3)

For grass on clay as well as grass on sand, the median and standard deviation of the U_c obtained with the GPT are lower than the median and standard deviation obtained with the WOS. For species-rich, the median U_c obtained with the GPT is lower than the (lower bound) median U_c obtained with the WOS, whereas the standard deviation is higher. However, the statistics obtained with the WOS are based on only three site so may not be true for the entire population.

6.3 Reconsideration of design choices and suggestions for future adaptations to the GPT

From the comparison of the U_c obtained with the GPT and WOS, the GPT seems to give a lower estimate of the U_c than the WOS. To improve the correspondence between GPT and WOS in future work, this section outlines several possible causes for the discrepancy between both methods and ways to improve the GPT.

Using the current GPT, it is assumed that the 30 samples of $\sigma_{grass,c}$ are sampled from a normal distribution, of which the 2.5th percentile represents the weakest spot. This 2.5th percentile is then implemented for $\sigma_{grass,c}(0)$ in Equation (5) to estimate U_c. Using this assumption, Bijlard et al. (2017) reported a good correspondence between the U_c obtained with the GPT and WOS. To test the applicability of the 2.5th percentile for skewed (i.e. non-normal) distributions, Figure 8 shows a synthetic 'grass pull test' through the use of random fields (Fenton, 2014). For every instance (B-D), 30 samples (orange) are taken from a spatially varying field of $\sigma_{grass,c}$, within a rectangular test plot of 10 by 15 m^2 (example in A). The values for constructing the random fields are sampled from the (lognormal) distribution of all individual $\sigma_{grass,c}$ values obtained in Future Dikes (n=20*30=600, mean = 1.0 N/cm^2, standard deviation = 0.3 N/cm^2, skewness = 0.5). The correlation length of the fields is set at roughly 3 m. This is rather arbitrary but sufficient for the purpose of visualization. Figure 8B shows an example of a field and sample distribution which are both positively skewed. Although the distributions in Figure 8B cannot be characterized as a normal distribution, which would require a skew of near 0, the 2.5th percentile roughly corresponds to the minimum field value. This indicates that the 2.5th percentile of a fitted normal distribution through the sample data may be representative for the weakest spot in the test plot over a wider range of skewness values.

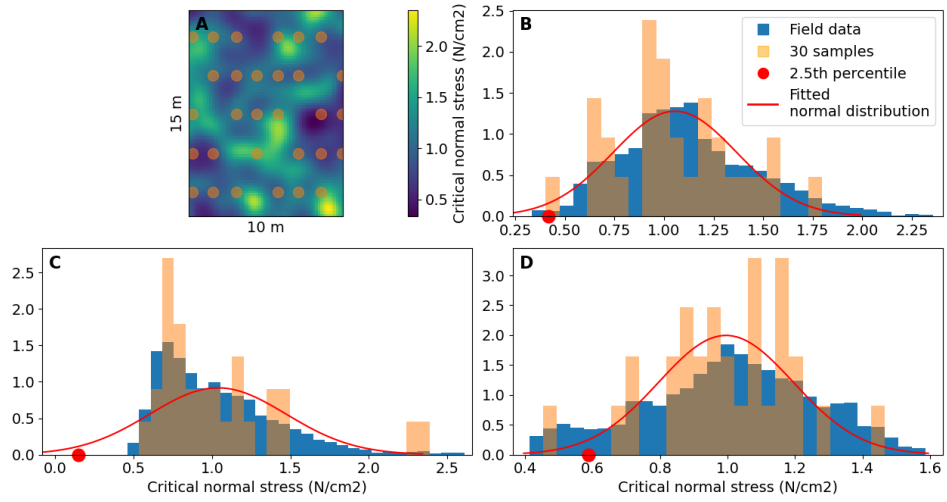

Figure 8 (A) Example of a synthetic test plot for the GPT. Sample locations of the GPT given in orange. (B) Field (skew = 0.52) and sample (skew = 0.26) histogram with a moderate positive skew. (C) Field (skew = 1.13) and sample (skew = 1.73) histogram with a strong positive skew. (D) Field (skew = -0.20) and sample (skew = -0.38) histogram with a negative skew.

However, the suitability of the 2.5th percentile of a normal distribution as a measure for the weakest spot seems to have limits. Figure 8C shows an example of a field and sample distribution which both have a strong positive skewness. In this case, the 2.5th percentile significantly underestimates the minimum field value. Figure 8D shows an example of a negatively skewed field and sample distribution, of which the 2.5th percentile overestimates the minimum field value. These examples indicate that the shape of the field and sample distribution may have an influence on the correspondence between the 2.5th percentile of the fitted normal distribution and the minimum field value. In future work, a more elaborate ensemble analysis using a large number of these random fields may reveal whether these observations are generally applicable. Subsequently, alternative design values or theoretical sample distributions may be used to improve the accuracy of the GPT for various (non-normal) distribution shapes.

Given the good correspondence between the GPT and WOS for the tests in Bijlard et al. (2017), the adoption of the real sod dimensions instead of the default dimensions to derive $\sigma_{grass,c}$ may be reconsidered. Besides the comparison between the U_c obtained with the GPT and WOS, $\sigma_{grass,c}$ itself may be validated by comparative testing with other types of grass pullout tests. For instance, a device developed for the EcoDike project in Germany measures the maximum tensile force of an intact grass sod and $\sigma_{grass,c}$ by anchoring a gypsum block to the above-ground parts of the vegetation (Michalzik et al., 2018, 2019).

Alternatively, to remove the uncertainty from measuring the sod dimensions to derive $\sigma_{grass,c}$, it may be desirable to exclude $\sigma_{grass,c}$ from the method entirely. This may be achieved by implementing the maximum tensile strength of an intact sod directly into the vertical force balance used in Hoffmans (2012). At the moment of failure of the grass sod during a GPT, the force balance looks as follows:

$$F_{upward,intact\ sod} \geq 4F_{shear,side} + F_{tensile,bottom} + F_{weight} \tag{6}$$

wherein the upward pull force exceeds the combination of shear forces from the four sides, the tensile force at the bottom and the own weight of the sod. The force balance can be translated to a stress balance by dividing the upward force by the area of the pull frame (A_f, 20 x 20 cm^2), the normal downward forces by the area of the bottom of the sod (A_b) and the shear force by the area of the sides (A_s):

$$\frac{F_{upward,intact\ sod}}{A_f} \geq \frac{(F_{weight} + F_{tensile,bottom})}{A_b} + \frac{4F_{shear,side}}{A_s} \tag{7}$$

obtaining:

$$\sigma_{upward} \geq \sigma_{bottom} + 4\sigma_{side} \tag{8}$$

The strength term on the right in Equation (8) represents the $\sigma_{grass,c}$ parameter which is used to determine U_c. However, since Equation (8) considers an equilibrium situation, the load term on the left may also be used to determine U_c. Using the shear stress balance ($\tau_0 > \tau_c$ with $\tau_c = \psi_c \sigma_{upward}$) in Hoffmans (2012), gives the following alternative formula for U_c:

$$U_c = \alpha_0 r_0^{-1} \sqrt{\frac{\psi_c(\sigma_{upward} - p_w)}{\rho_w}} \tag{9}$$

where α_0 (-) is a factor with value 1.2, σ_{upward} is equal to $F_i/(20x20)$ (N/cm^2), and all other parameters as defined before, see Equation (5). By using Equation (9) instead of (5), the interpretability of the GPT may be improved since U_c is only dependent on the maximum tensile force.

To test and validate (combinations of) these (and other) future adaptations to the GPT, it is important to include all historical tests for different types of vegetation and substrate. This way, a generally applicable method may be obtained that reliably estimates the U_c for species-rich as well as conventional grass covers.

Finally, future studies may focus on the more accurate determination of the relative turbulence intensity (r_0), the sampling strategy within the test plot, the degree of spatial correlation between the samples and the consequences for the observed sample distribution, as well as correlations of the tensile strength with soil and vegetation characteristics.

7 CONCLUSIONS

The aim of this paper was to assess the suitability of the grass pullout test (GPT) for quantitative erodibility assessment of grassed dike covers. For three species-rich dikes in the Netherlands, comparative tests with the GPT and wave overtopping simulator (WOS) were performed to assess the correspondence between the critical velocity (U_c) as derived with both methods.

The grass covers tested with the WOS did not fail, so only a lower bound of the U_c could be derived. The U_c obtained with the GPT is around the lower bound values derived with the WOS, which indicates that the estimates of the GPT are conservative. A similar conclusion can be drawn based on the comparison between the GPT and WOS on conventional grass covers with clayey and sandy substrates.

Hence, it can be concluded that the GPT is not yet fully suitable for accurate quantitative assessment of grass cover erodibility. Adaptations to the method are desired to improve the correspondence between the U_c derived with the GPT and the WOS. To obtain a generally applicable method, future adaptions should be tested and validated for conventional as well as species-rich grass covers with different substrates.

ACKNOWLEDGEMENT

Future Dikes is funded by the Dutch Flood Protection Program (Dutch: Hoogwaterbeschermingsprogramma, HWBP). Waterboard Rivierenland fulfils the role of client. The project is carried out by a consortium consisting of Radboud University Nijmegen, Wageningen Environmental Research, University of Twente, Infram Hydren, Eureco Advies, Deltares and Lumbricus Environmental Research and Consultancy.

REFERENCES

Bijlard, R., Steendam, G., Verhagen, H., & Van der Meer, J. (2017). Determining the critical velocity of grass sods for wave overtopping by a grass pulling device. C*oastal Engineering Proceedings*, *1*(35). https://doi.org/10.9753/icce.v35.structures.20

Hoffmans, G., Akkerman, G. J., Verheij, H., Van Hoven, A., & Van der Meer, J. (2009). The erodibility of grassed inner dike slopes against wave overtopping. *Coastal Engineering 2008*, *1*, 3224–3236. https://doi.org/10.1142/9789814277426_0267

Hoffmans, G. J. C. M. (2012). *The influence of turbulence on soil erosion*. Eburon. Utrecht. ISBN: 9789059726826

Hoffmans, G., Van Hoven, A., Steendam, G., & Van der Meer, J. (2018). Summary of research work about erodibility of grass revetments on dikes. *Protections 2018 (3rd International Conference on Protection against Overtopping), 6-8 June 2018*. Grange-over-Sands, UK. https://eprints.hrwallingford.com/1296/1/33_G_Hoffmans.pdf

Fenton, G. A. (2014). *Random Fields: Modeling Soil Properties*. In *Stochastic Analysis and Inverse Modeling* (pp. 95–109). The Alliance of Laboratories in Europe for Research and Technology. Grenoble. ISBN: 978-2-9542517-5-2. https://alertgeomaterials.eu/data/school/2014/2014_ALERT_schoolbook.pdf

Le, H.T., Van der Meer, Schiereck, G.J., Minh Cat, V., & Van der Meer, G. (2011). Wave overtopping simulator tests in Vietnam. *Coastal Engineering Proceedings*, *1*(32), 2. https://doi.org/10.9753/icce.v32.structures.2

Michalzik, J., Liebisch, S., & Schlurmann, T. (2018). Effects of Wave Load on the Long-Term Vegetation Development and its Resistance as Grass Revetments on Sea Dikes (Presentation). *36th International Conference on Coastal Engineering (ICCE2018)*. Baltimore, Maryland, USA. https://www.researchgate.net/publication/327512900

Michalzik, J., Liebisch, S., & Schlurmann, T. (2019). Development of an Outdoor Wave Basin to Conduct Long-Term Model Tests with Real Vegetation for Green Coastal Infrastructures. *Journal of Marine Science and Engineering*, *7*(1), 18. https://doi.org/10.3390/jmse7010018

Radboud University. (2023). *Future Dikes - How to strengthen the Dutch dikes with a species-rich grass covering*. [Online]. Available: https://www.ru.nl/en/research/research-projects/future-dikes [19-01-2023]

Steendam, G. J., Hoffmans, G., Bakker, J., Van der Meer, J., Frissel, J., Paulissen, M., & Verheij, H. (2012). *SBW Wave overtopping and grass cover strength - model development*. Deltares. Delft. https://repository.tudelft.nl/islandora/object/uuid:a9c99388-cf18-41db-b023-8e70dbae47f6/datastream/OBJ/download

Thornton, C., Van der Meer, J., Scholl, B., Hughes, S., & Abt, S. (2013). Testing levee slope resiliency at the new Colorado State University wave overtopping test facility. *Coastal Structures 2011*, 167–178. https://doi.org/10.1142/9789814412216_0015

Van Bergeijk, V. M., Warmink, J. J., & Hulscher, S. J. M. H. (2020). Modelling the Wave Overtopping Flow over the Crest and the Landward Slope of Grass-Covered Flood Defences. *Journal of Marine Science and Engineering*, *8*(7), 489. https://doi.org/10.3390/jmse8070489

Van der Meer, J. W., Bernardini, P., Snijders, W., & Regeling, E. (2007). The wave overtopping simulator. *Coastal Engineering 2006*, 4654–4666. https://doi.org/10.1142/9789812709554_0390

Van der Meer, J. W., Steendam, G. J., & Van Hoven, A. (2017). Validation of the Cumulative Overload Method Based on Tests by a New Wave Run-Up Simulator. *Coastal Structures and Solutions to Coastal Disasters Joint Conference 2015: Resilient Coastal Communities*, Boston, Massachusetts, USA. 731–742. https://doi.org/10.1061/9780784480304.077

Van der Meer, J.W., Allsop, N.W.H., Bruce, T., De Rouck, J., Kortenhaus, A., Pullen, T., Schüttrumpf, H., Troch, P. & Zanuttigh, B. (2018). *EurOtop. Manual on wave overtopping of sea defences and related structures*. An overtopping manual largely based on European research, but for worldwide application. www.overtopping-manual.com

Van der Meer, J. W. , Steendam, G. J., Mosca, C. A., Guzzo, L. B., Takata, K., Cheong, N. S., Eng, C. K., LJ, L. A., Ling, G. P., Siang, C. W., Seng, C. W., Karthikeyan, M., SC, F. Y., & Govindasamy, V. (2020). Wave overtopping tests to determine tropical grass species and topsoils for polder dikes in a tropical country. *Coastal Engineering Proceedings, (36v)*. https://doi.org/10.9753/icce.v36v.papers.31

Van Hoven, A. (2022). *Eindadvies beoordeling gras op zandbekledingen*. Deltares. Delft. Deltares document number: 11204369-002-GEO-009.